

From \mathbb{Z}_3 Rabi model to Potts model

Anatoliy I. Lotkov,¹ Denis V. Kurlov,¹ Valerii K. Kozin,¹ Jelena Klinovaja,¹ and Daniel Loss¹

¹*Department of Physics, University of Basel, Klingelbergstrasse 81, CH-4056 Basel, Switzerland*

We derive an exact mapping between a qubit-boson ring with momentum-dependent spin exchange and a 1-mode \mathbb{Z}_3 Rabi model. A canonical transformation yields closed-form expressions for the spectrum and shows that the three lowest eigenstates form orthogonal Schrödinger cat states, providing a naturally protected qutrit manifold. By coupling neighbouring Rabi units through number-conserving boson hopping we obtain an effective nearest-neighbour \mathbb{Z}_3 Potts Hamiltonian. For experimental implementation we present a dedicated superconducting-circuit design that uses charge qubits, LC resonators and Josephson junctions to realise both the qubit-boson and boson-boson couplings. We also translate our mapping to the optomechanical architecture introduced in the literature earlier. Parameter estimates and a disorder analysis confirm that the cat-state qutrit subspace remains well isolated under realistic conditions for both platforms.

I. INTRODUCTION

Systems with the \mathbb{Z}_n symmetry have sparked widespread interest across several areas of physics. In integrable systems research, the \mathbb{Z}_n symmetric Potts model plays an important role, being the non-trivial generalization of the simplest integrable systems like the Ising model or the XXZ model [1–4]. \mathbb{Z}_n symmetry also arises in topological phases: parafermionic edge modes—generalizations of Majorana modes—inherently arise naturally [5–7]. Finally, \mathbb{Z}_n symmetry is useful for applied quantum technology, where qudit-based processors extend the usual qubit paradigm [8–10]. Besides, modern platforms for quantum computations, such as trapped ions or superconducting qubits, inherently possess more than 2 energy levels that can be used for the computation. And systems based on n -level qudits unavoidably bear \mathbb{Z}_n symmetry.

For the sake of simplicity, we mostly discuss the \mathbb{Z}_3 symmetric case. Nevertheless, the results we obtained could be straightforwardly generalized to \mathbb{Z}_n case. The main topic of this paper is the \mathbb{Z}_3 Rabi model. The usual \mathbb{Z}_2 Rabi model being one of the simplest quantum models is ubiquitous in modern condensed matter physics [11–13]. Hence, it is only natural to study its \mathbb{Z}_n generalization, which has also been gaining traction [14–16]. We also talk about several variations of the \mathbb{Z}_3 Rabi model, their similarities and differences.

In particular, the model exhibits behavior similar to the superradiant phase found in the ordinary Rabi model. Although we have not formally proven this, we offer supporting evidence for the existence of this phase transition. In the relevant regime, the ground state becomes a n -fold generalization of the cat state. A renewed interest in cat state research has emerged due to its proposed application as a Quantum Error Correction Code [17–19]. Cat states based on a two-photon dissipation boson system were even proposed as a platform for fault-tolerant quantum computation [20]. However, cat-state-based quantum error correction was mostly discussed in the context of qubits. In this work, by achieving 3-fold cat states, we extend this concept to qudits.

We then present a method to experimentally implement the \mathbb{Z}_3 Rabi model in various physical platforms, illustrated by superconducting qubits. To our knowledge, it is the first proposal to realize the \mathbb{Z}_3 Rabi model experimentally. We utilize discrete rotational symmetry of 1-dimensional finite systems with periodic boundary conditions as a source of \mathbb{Z}_n symmetry. We also discuss why more straightforward approaches to implement the \mathbb{Z}_n Rabi model do not work.

Next, a generalization of Hwang’s proposal to build an Ising model by coupling a chain of \mathbb{Z}_2 Rabi models [21] allows us to combine a chain of \mathbb{Z}_3 Rabi models into a \mathbb{Z}_3 Potts model. As far as we know, quantum Potts models are also yet to be implemented in the experiment, except by simulating on a universal quantum computer. However, recently another realization based on Josephson junctions was proposed [22]. Hence, we believe our proposal could be of interest. Additionally, the Potts model is dual to a parafermion chain [23]. In particular, the chiral Potts model, i.e., a chain of Rabi models coupled chirally, exhibits already mentioned parafermion edge modes [24]. Although we only briefly touch on the parafermion edge modes in this paper, we believe that a further investigation in this direction could be fruitful.

In the remainder of the manuscript we proceed as follows. In Sec. II we introduce the **1-mode** \mathbb{Z}_3 Rabi model, derive a canonical transformation that considerably simplifies the model, and show that the three lowest eigenstates form mutually orthogonal three-fold cat states; **first-order perturbation theory then yields closed expressions for their splittings**. Sec. III generalises this construction to a **two-mode** version that exploits the hidden SU(2) symmetry of the two-dimensional harmonic oscillator; we obtain analytic spectra and identify a naturally protected “Rabi-qutrit” subspace that we use later. In Sec. IV, we outline two concrete realisations: a superconducting-circuit architecture based on charge qubits, LC resonators and Josephson junctions, and an optomechanical platform with trapped ions coupled through a chiral photonic ring; a step-by-step mapping shows how the required \mathbb{Z}_3 Rabi Hamiltonian emerges and why simpler routes fail. **Sec. V** couples

many such Rabi units through number-conserving boson hopping to derive an effective nearest-neighbour \mathbb{Z}_3 Potts chain; we give explicit circuit and optomechanical layouts, and discuss how a chiral variant realises parafermionic edge modes. Sec. VI analyzes the impact of realistic disorder: mis-aligned Zeeman fields that break spin-excitation conservation, and parameter inhomogeneities that break \mathbb{Z}_3 symmetry; numerical simulations confirm that the cat-state manifold remains well isolated for experimentally achievable levels of noise. Finally, Sec. VII summarises our key results and highlights future directions.

II. 1-MODE RABI MODEL

A. General definition

The \mathbb{Z}_2 Rabi model comprises a boson mode and a qubit mode with a \mathbb{Z}_2 symmetric interaction, where the \mathbb{Z}_2 symmetry restricted to boson mode is a subgroup of the $U(1)$ boson symmetry. To generalize it to the \mathbb{Z}_n case we consider a n -level system (qudit) instead of a qubit. The \mathbb{Z}_n symmetry action on the qudit is straightforward, on the other hand, its action on the boson is similarly to the \mathbb{Z}_2 case a subgroup of the $U(1)$ symmetry group. In this paper we would like to consider several variations of the \mathbb{Z}_n Rabi model with 1 or 2 boson modes.

The 1-mode \mathbb{Z}_n Rabi model [?] is:

$$\hat{H} = \Omega_R \hat{a}^\dagger \hat{a} + \sum_{j=1}^{n-1} B_j Z^j - \lambda(\hat{a} X^\dagger + \hat{a}^\dagger X), \quad (1)$$

where $B_j = B_{n-j}^*$. We use Z to denote the clock matrix, and X – the shift matrix. They are $n \times n$ matrices with elements being

$$Z_{ij} = \delta_{ij} \omega^{j-1}, \quad X_{ij} = \delta_{i-j+1 \bmod n, 0}, \quad (2)$$

where $\omega = \exp[2\pi i/n]$. Hereafter, we call the pure qudit term $\sum_j B_j Z^j$ a “magnetic” term, because its \mathbb{Z}_2 analogue is the Zeeman term.

We also define two bases in the qudit space: the one diagonalizing Z matrix $Z|j\rangle = \omega^j|j\rangle$, $j = 0, \dots, n-1$, and the one diagonalizing X matrix $X|\omega^k\rangle = \omega^k|\omega^k\rangle$, $k = 0, \dots, n-1$. They are related to each other by the discrete Fourier transform:

$$|\omega^k\rangle = \sum_{j=0}^{n-1} \omega^{-kj} |j\rangle. \quad (3)$$

As was already mentioned, the model has a \mathbb{Z}_n symmetry, which counts the number of boson-mode excitations and qudit excitations modulo n . In other words, one can think about the system as if there is an excitation hopping between boson and qudit degrees of freedom. The explicit form of the \mathbb{Z}_n symmetry generators is as follows:

$$\hat{R} = \exp \left[\frac{2\pi i}{n} \hat{a}^\dagger \hat{a} \right] \cdot Z. \quad (4)$$

More general \mathbb{Z}_n -symmetric variants of (1) are possible. In particular, terms $\hat{a}^2 X^2$, $(\hat{a}^\dagger)^2 (X^\dagger)^2$ can be added because they still conserve the number of excitation modulo n . However, it makes the system considerably more complicated, and we do not consider them in this paper.

B. \mathbb{Z}_3 definition

We focus on the \mathbb{Z}_3 Rabi model because its simpler notation keeps the central ideas transparent. For example, we do not need a summation in the Hamiltonian:

$$\hat{H}_{R1} = \Omega_R \hat{a}^\dagger \hat{a} + B(e^{i\phi} Z + e^{-i\phi} Z^\dagger) - \lambda(\hat{a}^\dagger X + \hat{a} X^\dagger). \quad (5)$$

We have added the subscript “R1” to the Hamiltonian to emphasize that this represents a 1-mode \mathbb{Z}_3 Rabi model, distinguishing it from the 2-mode \mathbb{Z}_3 Rabi model discussed in the next section.

In the \mathbb{Z}_3 case the explicit form of X , Z matrices is:

$$X = \begin{pmatrix} 0 & 0 & 1 \\ 1 & 0 & 0 \\ 0 & 1 & 0 \end{pmatrix}, \quad Z = \begin{pmatrix} 1 & 0 & 0 \\ 0 & \omega & 0 \\ 0 & 0 & \omega^2 \end{pmatrix}. \quad (6)$$

Alternatively, it is possible to present the Hamiltonian (5) as a 3×3 matrix:

$$\hat{H}_{R1} = \begin{pmatrix} \Omega_R \hat{a}^\dagger \hat{a} + \epsilon_0 & -\lambda \hat{a}^\dagger & -\lambda \hat{a} \\ -\lambda \hat{a} & \Omega_R \hat{a}^\dagger \hat{a} + \epsilon_1 & -\lambda \hat{a}^\dagger \\ -\lambda \hat{a}^\dagger & -\lambda \hat{a} & \Omega_R \hat{a}^\dagger \hat{a} + \epsilon_2 \end{pmatrix}, \quad (7)$$

where $\epsilon_k = 2B \cos(\phi + 2\pi k/3)$, $k = 0, 1, 2$. The symmetry generator is straightforwardly obtained from Eq. 4:

$$\hat{R}_{R1} = \exp \left[\frac{2\pi i}{3} \hat{a}^\dagger \hat{a} \right] \cdot Z. \quad (8)$$

Henceforth, \hat{X} , \hat{Z} , \hat{R} exclusively mean the \mathbb{Z}_3 case operators.

C. Canonical transformation

While different ways exist to demonstrate the existence of cat-state like ground states in the \mathbb{Z}_3 Rabi model (they are the same as in \mathbb{Z}_2 Rabi mode) like a variational method [?] or Schrieffer-Wolff transformation to decouple spin variable [?], we find the following approach to be the most simple and transparent.

It is a generalization of a known idea in the \mathbb{Z}_2 Rabi model [?]. We employ a canonical transformation that decouples qudit from boson degrees of freedom:

$$\hat{b} = \hat{a} X^\dagger, \quad \hat{b}^\dagger = \hat{a}^\dagger X. \quad (9)$$

The newly introduced boson creation/annihilation operators satisfy the necessary commutation relations:

$$[\hat{b}, \hat{b}^\dagger] = X[\hat{a}, \hat{a}^\dagger]X^\dagger = 1. \quad (10)$$

However, they do not commute with qutrit operators now. We next eliminate the spin operators altogether. First of all, the harmonic oscillator term and the interaction term could be easily expressed using new operators:

$$\begin{aligned} \Omega_R \hat{a}^\dagger \hat{a} - \lambda(\hat{a}^\dagger X + \hat{a} X^\dagger) \\ = \Omega_R(\hat{b}^\dagger - \lambda/\Omega_R)(\hat{b} - \lambda/\Omega_R) - \lambda^2/\Omega_R \end{aligned} \quad (11)$$

This yields a shifted harmonic oscillator as a result.

However, we are still left with the “magnetic” term $B(e^{i\phi}Z + e^{-i\phi}Z^\dagger)$. It is also feasible to express it using \hat{b} , \hat{b}^\dagger . To achieve this we decompose the Hilbert space into three subspaces with a fixed \mathbb{Z}_3 parity: $\mathcal{H} = \mathcal{H}_0 \oplus \mathcal{H}_1 \oplus \mathcal{H}_2$, where R when restricted to each of these subspaces is proportional to an identity operator:

$$R|_{\text{Rabi}}|_{\mathcal{H}_k} = \omega^k. \quad (12)$$

After substituting the definition of \mathbb{Z}_3 symmetry operator \hat{R} into Eq. 12, we can express the spin variable \hat{Z} as

$$\hat{Z}|_{\mathcal{H}_k} = \omega^k \exp\left(-\frac{2\pi i}{3}\hat{a}^\dagger \hat{a}\right)\Big|_{\mathcal{H}_k} = \omega^k \exp\left(-\frac{2\pi i}{3}\hat{b}^\dagger \hat{b}\right)\Big|_{\mathcal{H}_k} \quad (13)$$

The expressions are similar for different subspaces \mathcal{H}_k , and the subspace number k affects only the complex phase. Using this expression it is possible to express the “magnetic” term in Hamiltonian using the new boson creation/annihilation operators:

$$(e^{i\phi}Z + e^{-i\phi}Z^\dagger)|_{\mathcal{H}_k} = 2\cos\left[\frac{2\pi}{3}(\hat{b}^\dagger \hat{b} - k) - \phi\right]|_{\mathcal{H}_k}. \quad (14)$$

Finally, we can express the full \mathbb{Z}_3 Rabi model Hamiltonian using the \hat{b} and \hat{b}^\dagger operators:

$$\begin{aligned} \hat{H}_{\text{Rabi}}|_{\mathcal{H}_k} = \Omega_R(\hat{b}^\dagger - \lambda/\Omega_R)(\hat{b} - \lambda/\Omega_R) - \lambda^2/\Omega_R \\ + 2B\cos\left[\frac{2\pi}{3}(\hat{b}^\dagger \hat{b} - k) - \phi\right]. \end{aligned} \quad (15)$$

It is still not easy to find the exact eigenstates. However, approximate solutions provided by perturbation theory are sufficient for our purposes.

D. Perturbation theory

The Hamiltonian can be divided into unperturbed and perturbative parts,

$$\begin{aligned} \hat{H}_{\text{R1}}|_{\mathcal{H}_k} &= \hat{H}_{\text{R1},0} + \hat{H}_{\text{R1,pert}}, \\ \hat{H}_{\text{R1},0} &= \Omega_R(\hat{b}^\dagger - \lambda/\Omega_R)(\hat{b} - \lambda/\Omega_R) - \lambda^2/\Omega_R, \\ \hat{H}_{\text{R1,pert}} &= 2B\cos\left[\frac{2\pi}{3}(\hat{b}^\dagger \hat{b} - k) - \phi\right]. \end{aligned} \quad (16)$$

As we have already mentioned, the unperturbed Hamiltonian is just a shifted harmonic oscillator. As a result

its ground state in every \mathbb{Z}_3 sector is a coherent state [?]

$$\begin{aligned} |\psi_k\rangle &= |\lambda/\Omega_R\rangle_{\hat{b},k}, \text{ where} \\ \hat{b}|\lambda/\Omega_R\rangle_{\hat{b},k} &= (\lambda/\Omega_R)|\lambda/\Omega_R\rangle_{\hat{b},k}, \\ \hat{R}|\lambda/\Omega_R\rangle_{\hat{b},k} &= \omega^k|\lambda/\Omega_R\rangle_{\hat{b},k}. \end{aligned} \quad (17)$$

In terms of the original degrees of freedom, the states $|\psi_k\rangle$ turn out to be threefold cat-state:

$$\begin{aligned} |\psi_k\rangle &= \frac{1}{\sqrt{3}}[|\lambda/\Omega_R\rangle_{\hat{a}}|\omega^0\rangle + \omega^k|\omega\lambda/\Omega_R\rangle_{\hat{a}}|\omega^2\rangle \\ &\quad + \omega^{2k}|\omega^2\lambda/\Omega_R\rangle_{\hat{a}}|\omega\rangle]. \end{aligned} \quad (18)$$

Here, we again can see a parallel with the \mathbb{Z}_2 Rabi model, whose ground states are the usual cat states.

In general, a complex interaction coupling λ might be considered. This leads to a ground state of the unperturbed Hamiltonian being a coherent state with a complex parameter. Although considering a more general case of the complex λ could be beneficial, we do not need it for our purposes in this paper. Therefore, we assume that λ is real.

Next, we use the perturbation $\hat{H}_{\text{R1,pert}}$ to lift the degeneracy of $|\psi_k\rangle$. This is crucial for us, as we intend to utilize these states as a basis for the \mathbb{Z}_3 Potts model. Although the three states $|\psi_k\rangle, k = 0, 1, 2$, are degenerate eigenstates of the unperturbed Hamiltonian, they still constitute the natural degenerate-perturbation-theory basis: each $|\psi_k\rangle$ is an eigenstate of the \mathbb{Z}_3 symmetry operator \hat{R} with different eigenvalues, and the perturbation $\hat{H}_{\text{R1,pert}}$ commutes with \hat{R} . Because of this symmetry, $\hat{H}_{\text{R1,pert}}$ cannot mix these states, making them the correct choice for evaluating the first-order perturbation theory. We take the limit $B \ll \Omega_R$ to make the perturbation theory correction to $|\psi_k\rangle$ negligible. The corrections to the eigenenergies are:

$$\begin{aligned} \epsilon_k \delta_{kl} &= \langle \psi_k | \hat{H}_{\text{R1,pert}} | \psi_l \rangle \\ &= 2Be^{-\frac{3}{2}(\lambda/\Omega_R)^2} \cos\left[\frac{2\pi k}{3} + \phi - \frac{\sqrt{3}}{2}(\lambda^2/\Omega_R^2)\right] \delta_{kl}. \end{aligned} \quad (19)$$

The comparison with the numerical data is shown in Fig. 1. This comparison shows that the first-order perturbation theory works well. Besides, this is an improvement over the variational method used in [?], which generated the correct eigenvalues only for $\lambda > 0.61$.

III. 2-MODE RABI MODEL

A. Definition

This paper focuses primarily on a particular 2-mode \mathbb{Z}_3 Rabi model, as the section IV A outlines a potential

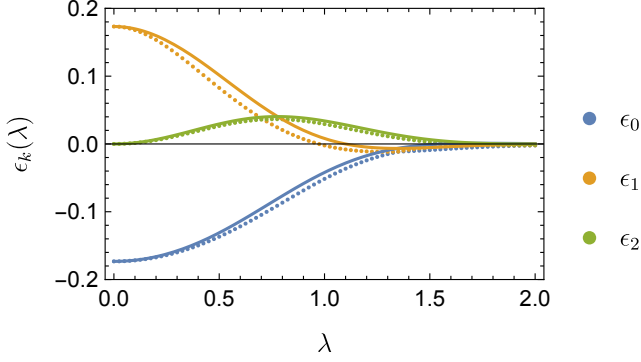


FIG. 1. Eigenvalues ϵ_k of the 1-mode \mathbb{Z}_3 Rabi model Hamiltonian \hat{H}_{R1} (5) as a function of coupling λ are depicted (both variables are plotted in units of Ω_R). The dotted line represents numerical results, while the solid line corresponds to the first-order perturbation theory (19). We see that the perturbation theory matches the numerics well. Parameters used: $\Omega_R = 1$, $B = 0.1$, $\phi = 7\pi/6$.

approach by which it could be realized experimentally. The Hamiltonian for this 2-mode \mathbb{Z}_3 Rabi model is:

$$\begin{aligned} \hat{H}_{R2} = & \Omega_R(\hat{a}_1^\dagger \hat{a}_1 + \hat{a}_2^\dagger \hat{a}_2) + B(e^{i\phi} Z + e^{-i\phi} Z^\dagger) \\ & - \lambda(\hat{a}_1 + \hat{a}_2^\dagger)X - \lambda(\hat{a}_1^\dagger + \hat{a}_2)X^\dagger. \end{aligned} \quad (20)$$

The Hamiltonian subscript “R2” is again necessary to distinguish the 2-mode Rabi model Hamiltonian from the 1-mode Rabi model Hamiltonian \hat{H}_{R1} (5).

This model (20) is a natural extension of the 1-mode \mathbb{Z}_3 Rabi model (5), albeit with a certain asymmetry between the two modes. Specifically, in the interaction term, we have $(\hat{a}_1 + \hat{a}_2^\dagger) \cdot X + \text{h.c.}$, where the first mode couples via an annihilation operator, and the second mode couples via a creation operator. Another possible 2-mode extension of the 1-mode \mathbb{Z}_3 Rabi model \hat{H}_{R1} (5) with the interaction term $(\hat{a}_1^\dagger + \hat{a}_2^\dagger)X + \text{h.c.}$ is discussed in Appendix B. However, this 2-mode variation turns out to be in a certain sense trivial. It has the same eigenvalues as the 1-mode Rabi model but with an additional degeneracy.

The \mathbb{Z}_3 symmetry generator has the following form:

$$\hat{R}_{R2} = \exp\left[\frac{2\pi i}{3}\hat{L}_3\right] \cdot Z, \text{ with } \hat{L}_3 = \hat{a}_1^\dagger \hat{a}_1 - \hat{a}_2^\dagger \hat{a}_2, \quad (21)$$

where \hat{L}_3 is a generator of the 2-dimensional quantum harmonic oscillator $SU(2)$ symmetry. (see App. A). Hence, the boson part of the \mathbb{Z}_3 symmetry is a residual part of the $SU(2)$ symmetry present in the 2-dimensional quantum harmonic oscillator.

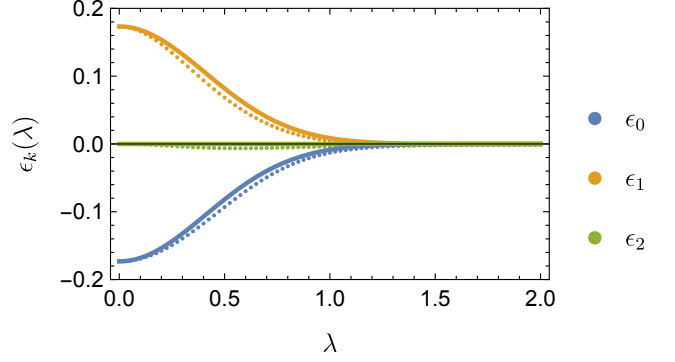


FIG. 2. Eigenvalues ϵ_k of the 2-mode \mathbb{Z}_3 Rabi model (20) as functions of coupling λ are depicted (both variables are plotted in the units of Ω_R). The dotted line represents numerical results, while the solid line corresponds to the first-order perturbation theory (26). The figure shows that the numerical and the perturbation-theory results are very close. Parameters used: $\Omega_R = 1$, $B = 0.1$, $\phi = 7\pi/6$.

B. Equivalent model

The 2-mode Rabi model (20) is equivalent to the Rabi model considered in Ref. [?]:

$$\begin{aligned} \hat{H}_{R2'} = & \Omega_R(\hat{a}_1^\dagger \hat{a}_1 + \hat{a}_2^\dagger \hat{a}_2) + B(e^{i\phi} Z + e^{-i\phi} Z^\dagger) \\ & - \lambda(\hat{x}_1 + i\hat{x}_2)\hat{X} - \lambda(\hat{x}_1 - i\hat{x}_2)X^\dagger, \end{aligned} \quad (22)$$

here we define $x_{1,2} = (a_{1,2} + a_{1,2}^\dagger)/\sqrt{2}$. This representation of the 2-mode \mathbb{Z}_3 Rabi model can be transformed into our \hat{H}_{R2} (20) by a canonical transformation mixing the two boson modes. The \mathbb{Z}_3 symmetry generator in this case takes the form:

$$R_{R2'} = \exp\left[\frac{2\pi i}{3}(\hat{x}_1 \hat{p}_2 - \hat{x}_2 \hat{p}_1)\right] \otimes Z \quad (23)$$

As one can see, in this 2-mode \mathbb{Z}_3 Rabi model the \mathbb{Z}_3 symmetry is realized in a peculiar way. The boson part of the \mathbb{Z}_3 symmetry generator is just a discrete rotation in the plane of the 2-dimensional harmonic quantum oscillator.

C. Spectrum

The method we used to find the spectrum of the 1-mode \mathbb{Z}_3 Rabi model still works for the 2-mode case with slight changes. Once again, we introduce new boson operators $\hat{b}_1 = \hat{a}_1 X$, $\hat{b}_2 = \hat{a}_2 X^\dagger$. Considering the different parity sectors separately, we rewrite the Hamiltonian (20) in terms of the new boson operators:

$$\begin{aligned} \hat{H}_{R2}|_{\mathcal{H}_k} = & \Omega_R \sum_i (\hat{b}_i^\dagger - \lambda/\Omega_R)(\hat{b}_i - \lambda/\Omega_R) - 2\lambda^2/\Omega_R \\ & + 2B \cos\left[\frac{2\pi}{3}(\hat{L}_z - k) - \phi\right] \end{aligned} \quad (24)$$

Consequently, we have 2 shifted QHO with a parity-dependent perturbation. The ground states in each sector are similarly easy to find:

$$|\psi_k\rangle = \frac{1}{\sqrt{3}} \sum_{l=0}^2 \omega^{lk} |\omega^{-l} \lambda / \Omega_R\rangle_{\hat{a}_1} |\omega^l \lambda / \Omega_R\rangle_{\hat{a}_2} |\omega^l\rangle. \quad (25)$$

Although the states $|\psi_k\rangle$ have their cat-state structure for any coupling strength, but it becomes physically meaningful only once the interaction reaches the deep-strong coupling regime $\lambda \gtrsim \Omega_R$ for $|\psi_k\rangle$, where the individual coherent-state components in (25) become well-separated.

As in the 1-mode \mathbb{Z}_3 Rabi model, the cat states $|\psi_k\rangle$ serve as a unique basis in the ground state of the shifted quantum oscillator with the specific \mathbb{Z}_3 parity: $\hat{R}|\psi_k\rangle = \omega^k |\psi_k\rangle$. For later convenience, we denote the subspace spanned by $|\psi_k\rangle$ by $\mathcal{R} = \text{Span}\{|\psi_k\rangle\}$. Because the perturbation commutes with \hat{R} , the symmetry labels prevent mixing between different k , making $|\psi_k\rangle$ the natural basis for degenerate perturbation theory. Once again, we consider the limit $B \ll \Omega_R$ to make the eigenstate corrections negligible. Using the first order perturbation theory we find the energy corrections:

$$\epsilon_k \delta_{kl} = \langle \psi_k | \hat{V} | \psi_l \rangle = 2B e^{-3(\lambda/\Omega_R)^2} \cos\left[\frac{2\pi k}{3} + \phi\right] \delta_{kl}. \quad (26)$$

Note that here the phase does not depend on the coherent state parameter. In Fig. 2 the analytical result is compared with the numerics.

The effective Hamiltonian for cat-states $|\psi_k\rangle$ is

$$\hat{H}_{R2}|_{\mathcal{R}} = \text{diag}[\epsilon_0, \epsilon_1, \epsilon_2] = \tilde{B}(e^{i\phi} Z_{\mathcal{R}} + e^{-i\phi} Z_{\mathcal{R}}^\dagger), \quad (27)$$

with $\tilde{B} = B e^{-3(\lambda/\Omega_R)^2}$. We introduced $Z_{\mathcal{R}}$ as a Z matrix acting in \mathcal{R} . This particular form of the Hamiltonian is later useful to construct the \mathbb{Z}_3 Potts model in Sec. V.

Cat states provide useful passive protection against phase noise. In qubit systems this protection can be extended to bit-flip errors by switching from the usual two-component cats to four-component ones [?]. The same idea carries over to the \mathbb{Z}_3 setting: the three-component cats that realise our qutrit already suppress phase noise, and embedding the logical qutrit in a six-component cat (as produced, for example, by a \mathbb{Z}_3 Rabi model) should also guard against flip errors. The larger Hilbert space can then be handled with standard stabiliser-code techniques to correct arbitrary single-qutrit errors. A full construction and performance analysis is left for future work.

To make a distinction with other 3-level systems considered in this paper we will below call the 3-dimensional Hilbert space \mathcal{R} spanned by the threefold cat states the Rabi qutrit. In particular, we use a chain of Rabi qutrits to create a Potts model in Sec. V.

IV. PHYSICAL IMPLEMENTATION

A. Qubit-boson ring

In this section, we describe a general strategy to physically implement the \mathbb{Z}_3 Rabi model. To this end, we use a qubit-boson ring (QB ring) with a specific qubit-boson interaction described below as a base system. Below, we will describe two distinct physical platforms to realize our proposed system on. The Hamiltonian of the QB ring is given by

$$\begin{aligned} \hat{H}_{QB} &= \epsilon \sum_{j=0}^2 \sigma_j^z + \Omega_{QB} \sum_{j=0}^2 \hat{a}_j^\dagger \hat{a}_j + \hat{V}_{QB}, \\ \hat{V}_{QB} &= g \sum_{j=0}^2 \left(\sigma_j^+ \sigma_{j+1}^- e^{i(\hat{x}_j - \hat{x}_{j+1})} + \text{h.c.} \right). \end{aligned} \quad (28)$$

In this section we are giving a short description of the correspondence between the qubit-boson ring (28) and the 2-mode Rabi model \hat{H}_{R2} (20). For a detailed discussion, we refer the reader to App. C.

Here we use the standard definition for the creation/annihilation operators:

$$\hat{a}_j = \sqrt{\frac{m_{QB} \Omega_{QB}}{2}} \hat{x}_j + i \sqrt{\frac{1}{2m_{QB} \Omega_{QB}}} \hat{p}_j, \quad (29)$$

where Ω_{QB} is the boson frequency and m_{QB} is the mass. It is a variant of the Hamiltonian considered in [?].

The Hamiltonian (28) commutes with the z -component of the total spin $\hat{S}^z = \sum_i \sigma_i^z$. Consequently, we consider the restriction of \hat{H}_{QB} to the sector with a single spin being up (and the rest being down) $\mathcal{H}_{QB,1}$ (detailed discussion in App. C). That is the sector described by the \mathbb{Z}_3 Rabi model.

However, first we need to transform the Hamiltonian (28) a bit. To begin with, we apply the momentum-translation operator $S = \prod_j \exp[i\sigma_j^z \hat{x}_j/2]$ to eliminate the exponential interaction term \hat{V} . As a result, we obtain

$$\begin{aligned} S^{-1} \hat{H}_{QB} S &= \epsilon \sum_{j=0}^2 \sigma_j^z + \Omega_{QB} \sum_{j=0}^2 \hat{a}_j^\dagger \hat{a}_j + \frac{1}{2m_{QB}} \sum_{j=0}^2 \hat{p}_j \sigma_j^z \\ &\quad + \frac{3}{4m_{QB}} + g \sum_{j=0}^2 (\sigma_j^+ \sigma_{j+1}^- + \sigma_j^- \sigma_{j+1}^+). \end{aligned} \quad (30)$$

The interaction \hat{V}_{QB} indeed simplified and turned into a pure qubit term (last term). On the other hand, we obtained a new boson-qubit interaction $\sum \hat{p}_j \sigma_j^z$.

The next step is an application of the Fourier transform to both qubit and boson operators [?]. It is important to note that the Fourier transform maps the sector \mathcal{H}_1 onto itself, because \hat{S}^z is invariant with respect to it. After the restriction to sector \mathcal{H}_1 , it leads to the decoupling of

one of the boson modes and simplifying the qubit operators. This way it simplifies the analysis. However, term $S^{-1}\hat{V}S$ is already well-prepared to the restriction to the \mathcal{H}_1 sector. Hence, we are leaving it intact.

$$\begin{aligned} S^{-1}\hat{H}_{QB}S = & \epsilon\sigma^z(0) + \Omega_{QB} \sum_{k=0}^2 \hat{a}^\dagger(k)\hat{a}(k) \\ & + \frac{i}{2} \sqrt{\frac{\Omega_{QB}}{2m_{QB}}} \sum_{k=0}^2 (-\hat{a}(k) + \hat{a}^\dagger(-k))\sigma^z(k) \\ & + g \sum_{j=0}^2 (\sigma_j^+ \sigma_{j+1}^- + \sigma_j^- \sigma_{j+1}^+) + \frac{3}{4m_{QB}}. \end{aligned} \quad (31)$$

Finally, we are ready to restrict the Hamiltonian to $\mathcal{H}_{QB,1} = \text{Span}[\{|\uparrow\downarrow\downarrow\rangle, |\downarrow\uparrow\downarrow\rangle, |\downarrow\downarrow\uparrow\rangle\}]$ sector. Only the qubit operators are influenced by the restriction. As was already said, the restriction to the single excitation sector leads to decoupling of the 0th boson mode $\hat{a}(0)$, $\hat{a}^\dagger(0)$. We leave it as well as constant terms out in the following.

$$\begin{aligned} \hat{H}_{QB,1} = & S^{-1}\hat{H}_{QB}S|_{\mathcal{H}_{QB,1}} \\ = & \Omega_{QB} \sum_{k=1}^2 \hat{a}^\dagger(k)\hat{a}(k) + g(X + X^\dagger) \\ & + i\sqrt{\frac{\Omega_{QB}}{6m_{QB}}} (-\hat{a}(1) + \hat{a}^\dagger(2))Z + \\ & i\sqrt{\frac{\Omega_{QB}}{6m_{QB}}} (-\hat{a}(2) + \hat{a}^\dagger(1))Z^2 \end{aligned} \quad (32)$$

To get the \mathbb{Z}_3 Rabi model in the form (20) we need to do some final fine-tuning. To be precise, we utilize the Hadamard transformation and the boson $U(1)$ symmetry to arrive to:

$$\begin{aligned} \hat{H}_{R2} = & U^{-1}\hat{H}_{QB,1}U \\ = & \Omega_{QB}(\hat{a}^\dagger(1)\hat{a}(1) + \hat{a}^\dagger(2)\hat{a}(2)) + g(Z + Z^\dagger) \\ & - \sqrt{\frac{\Omega_{QB}}{6m_{QB}}} (\hat{a}(1) + \hat{a}^\dagger(2))X \\ & - \sqrt{\frac{\Omega_{QB}}{6m_{QB}}} (\hat{a}(2) + \hat{a}^\dagger(1))X^\dagger, \end{aligned} \quad (33)$$

where the qubit-boson ring parameters relate to the \mathbb{Z}_3 Rabi model (20) parameters through the following mapping:

$$\Omega_R = \Omega_{QB}, B = g, \phi = 0, \lambda = \sqrt{\frac{\Omega_{QB}}{6m_{QB}}}. \quad (34)$$

As can be seen, the boson frequency remains the same while the Rabi interaction parameter λ is expressed by the combination of the boson frequency Ω_{QB} and the boson mass m_{QB} .

For clarity, we also write down the explicit form of the “magnetic” term,

$$g(Z + Z^\dagger) = \begin{pmatrix} 2g & 0 & 0 \\ 0 & -g & 0 \\ 0 & 0 & -g \end{pmatrix} \quad (35)$$

In the end, we see that the \mathbb{Z}_3 Rabi model describes the single-excitation sector of the boson-qubit ring (28).

We selected the superconducting qubits as the main platform to illustrate our proposal because it is relatively easy to engineer a superconducting circuit with the interaction we want. Moreover, the consequent analysis of the resulting quantum system is straightforward [? ? ?]. However, we believe that similar construction is also possible in other contexts. The optomechanical system is another example we provide.

1. Why so complicated?

The implementation of the \mathbb{Z}_3 Rabi model proposed in the previous section is considerably more complicated than the usual \mathbb{Z}_2 Rabi model implementations. To obtain the \mathbb{Z}_2 Rabi model it is enough to simply couple a qubit with a boson in a naive way. Therefore, one may wonder if these complications are needed. However, the straightforward generalization of the \mathbb{Z}_2 Rabi model to higher Rabi models does not work for rather profound reasons. It turns out to be considerably more difficult to get a \mathbb{Z}_3 symmetric interaction. In this section, we try to explain why.

There are two most common ways to get a two-level quantum system. It is possible to use a spin as a 2-level system [? ? ?] or two levels in anharmonic oscillator, e.g., the Rabi model describes a superconducting qubit coupled to a cavity in the ultra-strong coupling regime [? ? ? ? ?]. Therefore, it is simple to get a \mathbb{Z}_2 Rabi model. It is enough to take either a spin or an anharmonic oscillator and couple it to a boson mode using $\hat{V} = \sigma_x \hat{x}_{\text{boson}}$.

Both ways are easily generalized to the \mathbb{Z}_3 Rabi model. To get a spin-based 3-level system we just need to take spin 1. However, in this case, we obtain an interaction through the spin-1 representation of s^x instead of X .

$$s^x = \begin{pmatrix} 0 & \sqrt{2} & 0 \\ \sqrt{2} & 0 & \sqrt{2} \\ 0 & \sqrt{2} & 0 \end{pmatrix} \quad (36)$$

It is easy to see that it is not \mathbb{Z}_3 -symmetric. Hence, the spin 1/2 representation of the $SU(2)$ group is a convenient special case that, unfortunately, does not generalize. It does not mean that it is impossible to build a \mathbb{Z}_3 symmetric system out of spins as we have shown, or higher \mathbb{Z}_n symmetric systems [?] in general. But it still explains why we need rather complicated ways to achieve it.

The second way to get a \mathbb{Z}_2 Rabi model is to use 2 levels of an anharmonic oscillator. Consequently, in the \mathbb{Z}_2 case σ^x operator is basically a restriction of the coordinate operator of the anharmonic oscillator $\hat{x}_{\text{an}} = (\hat{a}_{\text{an}} + \hat{a}_{\text{an}}^\dagger)/\sqrt{2}$ to the two lowest levels. On the contrast, if we restrict it to 3-level system, we will get

$$\hat{x}_{\text{an}} = \frac{1}{\sqrt{2}} \begin{pmatrix} 0 & \sqrt{1} & 0 \\ \sqrt{1} & 0 & \sqrt{2} \\ 0 & \sqrt{2} & 0 \end{pmatrix} \quad (37)$$

As a result, the \mathbb{Z}_2 Rabi model based on the anharmonic oscillator does not generalize to the higher \mathbb{Z}_n Rabi models.

These obstacles make an experimental \mathbb{Z}_n -Rabi realization non-trivial, motivating our proposal.

The rationale provided in this section is in no way a formal proof. However, the argument should serve as an intuition as to why \mathbb{Z}_3 Rabi is less straightforward to engineer than its more well-known analogue. The model we proposed in the previous section solves this problem by having an inherent \mathbb{Z}_3 symmetry. It originates from the translational symmetry of a ring.

B. Superconducting circuit implementation

The obvious choice for boson modes is an LC circuit. For the qubit (σ_i) we consider superconducting charge qubits [? ? ? ?], because we want the qubit eigenstate to be a charge state. More extensive discussion on the charge qubits we use is provided in App. D. Here, we only want to comment that the qubit eigenstates are $|0\rangle, |1\rangle$ defined by $\hat{n}|0\rangle = 0$, $\hat{n}|1\rangle = |1\rangle$, where \hat{n} is the capacitor charge operator. Below, to denote a linear span of these states we use $\mathcal{V}_k = \text{Span}\{|0\rangle_k, |1\rangle_k\}$ where k is the number of the qubit.

Fig. 3 shows a superconducting realization of the three-site qubit-boson ring. Each site consists of an LC resonator ($C_{\text{Bsn}}, L_{\text{Bsn}}$) (C_B, L_B) that provides the bosonic mode and a charge qubit biased by a Josephson junction (JJ) with critical current I_Q and shunted by a capacitor with conductance C_Q . Nearest-neighbour qubit-boson coupling is introduced by additional Josephson junctions of critical current I_{Rabi} [? ? ? ?] that connect the qubits of site j and $j+1$. In practice the layout would incorporate read-out resonators, flux-bias lines, and filtering components, which are omitted here for clarity.

The JJ responsible for the interaction in the QB ring adds the following term to the Hamiltonian:

$$\hat{V}_{\text{SC QB},j} = I_{\text{Rabi}} \cos(\hat{\phi}_j + \hat{\varphi}_j - \hat{\phi}_{j+1} - \hat{\varphi}_{j+1}), \quad (38)$$

where ϕ_k is the k th LC circuit's flux, and φ_k is the k th charge qubit's superconducting phase.

As we are only interested in qubit states $|0\rangle_k, |1\rangle_k$, we restrict the JJ term $\hat{V}_{\text{SC QB},j}$ to the qubit Hilbert sub-

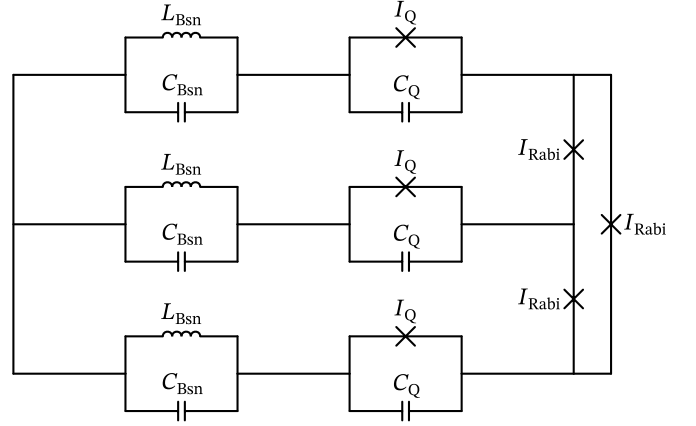


FIG. 3. Superconducting circuit implementation of the 2-mode \mathbb{Z}_3 Rabi model \hat{H}_{R2} . The LC circuits ($L_{\text{Bsn}}, C_{\text{Bsn}}$) host the boson modes; the charge qubits (I_Q, C_Q) correspond to the qubit degrees of freedom; Josephson junctions I_{Rabi} are responsible for the interaction term in the qubit-boson ring. Altogether the circuit is described by the Hamiltonian (28).

space $\mathcal{V}_j \otimes \mathcal{V}_{j+1}$:

$$\begin{aligned} \hat{V}_{\text{SC QB},j} \Big|_{\mathcal{V}_j \otimes \mathcal{V}_{j+1}} &= \\ &= \frac{I_{\text{Rabi}}}{2} \left(e^{i(\hat{\varphi}_j - \hat{\varphi}_{j+1})} e^{i(\hat{\phi}_j - \hat{\phi}_{j+1})} + h.c. \right) \Big|_{\mathcal{V}_j \otimes \mathcal{V}_{j+1}} \quad (39) \\ &= \frac{I_{\text{Rabi}}}{2} \left(e^{i(\hat{\varphi}_j - \hat{\varphi}_{j+1})} \sigma_j^- \sigma_{j+1}^+ + h.c. \right). \end{aligned}$$

Here we used the fact that $e^{\pm i\hat{\phi}}$ acts as a raising/lowering operator for the charge qubit: $e^{i\hat{\phi}}|_{\mathcal{V}} = \sigma^+$. This is exactly why specifically charge qubits are required, as opposed to flux or phase qubits.

In other words, the Josephson junction coupling between two pairs of an LC circuits and a charge qubits gives us precisely the interaction term we wanted. As a result, we conclude that the system depicted in Fig. 3 is described by the Hamiltonian (28). The qubit-boson ring couplings can be expressed by the circuit parameters:

$$\begin{aligned} \epsilon &= \frac{\delta}{2C_Q}, \quad \Omega_{QB} = \left(\sqrt{L_{\text{Bsn}} C_{\text{Bsn}}} \right)^{-1/2}, \\ m_{QB} &= C_{\text{Bsn}}, \quad g = \frac{I_{\text{Rabi}}}{2}. \end{aligned} \quad (40)$$

For details of the ϵ computation, consult App. D. Finally, applying Sec. IV A argument we deduce that the circuit is described by the \mathbb{Z}_3 Rabi model.

C. Optomechanical implementation

Another possible physical platform for the \mathbb{Z}_3 Rabi model is an optomechanical system consisting of 3 spins whose vibrational modes are boson degrees of freedom.

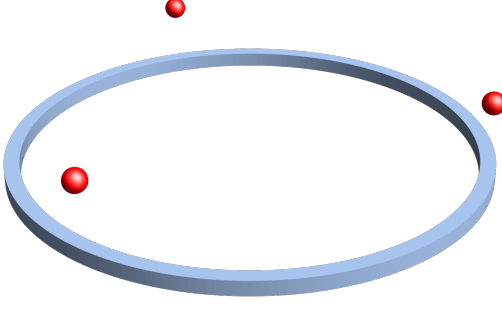


FIG. 4. Schematic illustration of the optomechanical implementation of the 2-mode \mathbb{Z}_3 Rabi model \hat{H}_{R2} [?] The red spheres are trapped ions carrying two-level systems; their vibrational modes are the bosons from the qubit-boson ring. The blue ring is the chiral waveguide that facilitates the interaction in the qubit-boson ring. The system is described by the Hamiltonian \hat{H}_{OM} (41).

They are connected by a circular waveguide that acts as an interaction medium between the spins and the vibrational phonons (first proposed in [?]).

Although experimentally realization of this system seems challenging, we still want to briefly talk about it to showcase the method we proposed in Sec. IV A on a different physical platform. In this section, we give a short explanation how the \mathbb{Z}_3 Rabi model appears in this model, for the extended discussion we refer the reader to the original paper [?].

The optomechanical model in question is described by the following Hamiltonian:

$$\begin{aligned}\hat{H}_{OM} &= \sum_{j=0}^2 \zeta_j \hat{c}_j^\dagger \hat{c}_j + \epsilon \sum_{j=0}^2 \sigma_j^z + \Omega_{OM} \sum_{j=0}^2 \hat{a}_j^\dagger \hat{a}_j + \hat{V}_{\text{int}}, \\ \hat{V}_{\text{int}} &= \gamma \sum_{k,j=0}^2 \left[\sigma_j^+ \hat{c}_k e^{ik[R\phi_j + \hat{x}_j]} + \text{h.c.} \right],\end{aligned}\quad (41)$$

where $\zeta_k = vk$.

Using the Schrieffer-Wolff transformation [?], we can integrate out the photons degrees of freedom to get the Hamiltonian in the form we want:

$$\begin{aligned}\hat{H}_{OM,\text{eff}} &= \epsilon \sum_j \sigma_j^z + \Omega_{OM} \sum_j \hat{a}_j^\dagger \hat{a}_j \\ &\quad - \frac{\gamma^2}{2v} \sum_{i < j} \left[i \sigma_i^+ \sigma_j^- e^{iqR\phi_{ij}} e^{i\eta(\hat{a}_i + \hat{a}_i^\dagger - \hat{a}_j - \hat{a}_j^\dagger)} + \text{h.c.} \right].\end{aligned}\quad (42)$$

The Hamiltonian is a bit different from (28). It is treated

in App. C and gives rise to the following \mathbb{Z}_3 Rabi model:

$$\begin{aligned}\hat{H}_{2\text{Rabi,mod}} &= -\frac{\gamma^2}{2v} (e^{-5\pi i/6} Z + e^{5\pi i/6} Z^\dagger) \\ &\quad + \Omega_{OM} (\hat{a}_1^\dagger \hat{a}_1 + \hat{a}_2^\dagger \hat{a}_2) \\ &\quad - \frac{\Omega_{OM}^{1/2} \eta}{6^{1/2}} \left[(\hat{a}_1 + \hat{a}_2^\dagger) X + (\hat{a}_2 + \hat{a}_1^\dagger) X^\dagger \right]\end{aligned}\quad (43)$$

which differs from the \mathbb{Z}_3 Rabi model we acquired in the superconducting circuit context only by the \mathbb{Z}_3 “magnetic” term’s phase $\varphi = -5\pi/6$.

We can explicitly write down the “magnetic” term

$$-\frac{\gamma^2}{2v} (e^{-5\pi i/6} Z + e^{5\pi i/6} Z^2) = \begin{pmatrix} \frac{\sqrt{3}\gamma^2}{2v} & 0 & 0 \\ 0 & -\frac{\sqrt{3}\gamma^2}{2v} & 0 \\ 0 & 0 & 0 \end{pmatrix}. \quad (44)$$

As one can see, the non-zero “magnetic” term’s phase φ leads to all the eigenvalues being non-degenerate. Compare it to Eq. (35).

V. POTTS MODEL FROM COUPLED \mathbb{Z}_3 RABI MODELS

A. Theoretical description

The \mathbb{Z}_3 Potts model [?] is a 1-dimensional chain of 3-level systems with a global \mathbb{Z}_3 symmetry. It originates from statistical physics as a straightforward generalization of the Ising model to more states on each site [? ?]. Nowadays, the Potts model often appears in the context of qudit quantum computations [? ?]. However, the direct experimental realization of the Potts model still does not exist. One of the goals of this paper is to propose such an experimental realization based on \mathbb{Z}_3 Rabi models. To achieve this, we generalize the idea of building an Ising model by coupling a chain of \mathbb{Z}_2 Rabi models, proposed by Hwang [?], to the \mathbb{Z}_3 -symmetric case. Below, we provide a thorough derivation.

The \mathbb{Z}_3 Potts model Hamiltonian is

$$\begin{aligned}\hat{H}_{\text{Potts}} &= f_{\text{Potts}} \sum_{n=1}^L (e^{i\phi} Z_n + e^{-i\phi} Z_n^\dagger) \\ &\quad + J_{\text{Potts}} \sum_{n=1}^L (X_n X_{n+1}^\dagger + X_n^\dagger X_{n+1}).\end{aligned}\quad (45)$$

The first term just describes single-excitation energies, the second term is the \mathbb{Z}_3 -symmetric nearest-neighbour interaction.

As we already discussed before, it is difficult to obtain a \mathbb{Z}_3 symmetry in an arbitrary 3-level system chain. But we have already learnt how to build a \mathbb{Z}_3 Rabi model. We use it as a building block for the \mathbb{Z}_3 Potts model, i.e., we want the 3 cat-states in the \mathbb{Z}_3 Rabi models (25) to serve as 3 states on the n th site of the Potts model

$|j\rangle_n = |\psi_j\rangle_n$ for $j = 0, 1, 2$. By raising boson energy Ω_R in the Rabi model Hamiltonian (20) the higher energy states are effective decoupled from $|\psi_j\rangle$ states.

The main reason why it is convenient to build the Potts model from Rabi models is that the boson degrees of freedom in the Rabi models allow us to obtain a \mathbb{Z}_3 symmetric interaction. The reasoning is simple; the Rabi model's \mathbb{Z}_3 symmetry acting on bosons is a residue of a usual $U(1)$ boson symmetry. Consequently, if we take a $U(1)$ symmetric interaction of boson modes on neighbor sites, then it will by default be \mathbb{Z}_3 symmetric. And the simplest $U(1)$ symmetric boson interaction is just a hopping term $\hat{a}_n^\dagger \hat{a}_{n+1} + \text{h.c.}$ As a result, to obtain a \mathbb{Z}_3 Potts model we need to take a chain of \mathbb{Z}_3 Rabi models and couple them by the boson hopping term:

$$\begin{aligned} \hat{H}_{\text{Rabi chain}} = & \\ \sum_{n=1}^L \hat{H}_{\text{Rabi},n} + J \sum_{n=1}^L \sum_{k=1}^2 & \left(\hat{a}_{n,k}^\dagger \hat{a}_{n+1,k} + \hat{a}_{n+1,k}^\dagger \hat{a}_{n,k} \right), \end{aligned} \quad (46)$$

where n is a chain-site subscript and k is a number of a boson mode in a \mathbb{Z}_3 Rabi model. We claim that this Hamiltonian gives us precisely the \mathbb{Z}_3 Potts model, when we restrict it to the Hilbert space $\bigotimes_n \mathcal{R}_n$ generated by the 3 cat states on the sites $n = 1, \dots, L$.

The action of $\hat{a}_{n,k}$ restricted to the Rabi qutrit is very simple:

$$\hat{a}_{n,k} |\psi_i\rangle_n = (\lambda/\Omega) |\psi_{i+1}\rangle_n. \quad (47)$$

For the creation operator it is a little bit more complicated:

$$\begin{aligned} \hat{a}_{n,k}^\dagger |\psi_i\rangle_n &= (\lambda/\Omega) |\psi_{i-1}\rangle_n + \delta, \text{ where} \\ |\delta|^2 &= 1. \end{aligned} \quad (48)$$

In the deep-strong coupling regime $\lambda/\Omega \gg 1$, we can neglect δ . As a result, in the Rabi qutrit subspace the creation/annihilation operators act as cyclic permutations: $\hat{a}_{n,k} |\mathcal{R}\rangle = (\lambda/\Omega) X$, $\hat{a}_{n,k}^\dagger |\mathcal{R}\rangle = (\lambda/\Omega) X^\dagger$. Consequently, in this sector the coupled Rabi chain is equivalent to the Potts model:

$$\begin{aligned} J \sum_{k=0}^2 & \left(\hat{a}_{n,k}^\dagger \hat{a}_{n+1,k} + \hat{a}_{n+1,k}^\dagger \hat{a}_{n,k} \right) = \\ 3(\lambda/\Omega)^2 J & \left(X_n^\dagger X_{n+1} + X_{n+1}^\dagger X_n \right). \end{aligned} \quad (49)$$

Therefore, we have $J_{\text{Potts}} = 3(\lambda/\Omega)^2 J$.

1. Underlying qubit-boson ring

Considering that the Rabi models in the chain are made from a qubit-boson ring, we need to show how to obtain the boson hopping interaction (??) in terms of the QB ring degrees of freedom.

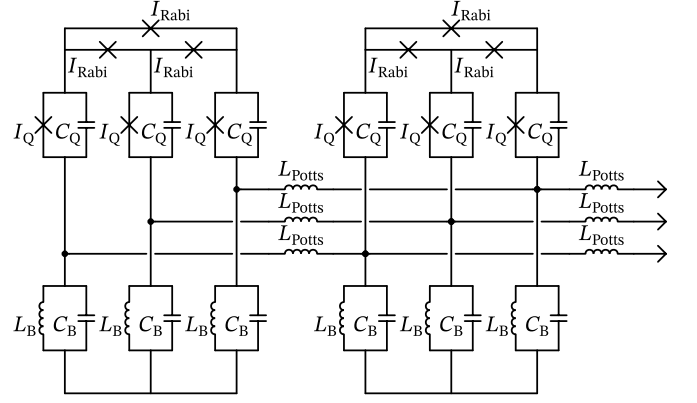


FIG. 5. Superconducting circuit implementation of the Potts model. The circuit is described by the Hamiltonian (46). Subscript “B” denote elements corresponding to boson degrees of freedom; subscript “Q” denote qubit elements; subscript “Rabi” denote elements responsible for interaction in qubit-boson ring; subscript “Potts” denote elements responsible for interaction in Potts model.

It turns out to be quite simple. If we add hopping terms for the bosons in the qubit-boson chain, then it will give us the hopping term between the Rabi model bosons, because the Fourier transform does not change the form of the boson hopping interaction:

$$\begin{aligned} & \sum_{j=0}^2 \left(\hat{a}_{n,j}^\dagger \hat{a}_{n+1,j} + \hat{a}_{n+1,j}^\dagger \hat{a}_{n,j} \right) \\ &= \sum_{k=0}^2 \left(\hat{a}_{n,k}^\dagger \hat{a}_{n+1,k} + \hat{a}_{n+1,k}^\dagger \hat{a}_{n,k} \right) \end{aligned} \quad (50)$$

To simplify the notation, we do not use brackets here to denote the Fourier components of the boson modes. The subscript j correspond to the real space boson mode; the subscript k corresponds to the Fourier boson mode, i.e., the \mathbb{Z}_3 Rabi model boson modes. We have an extra term $\hat{a}_{n,0}, \hat{a}_{n,0}^\dagger$ which decouples the same way it did in Sec. IV A.

The mapping between the parameters is the following:

$$\begin{aligned} f_{\text{Potts}} &= g \exp \left(-\frac{1}{2m_{QB}\Omega_{QB}} \right), \\ J_{\text{Potts}} &= \frac{J}{2m_{QB}\Omega_{QB}}. \end{aligned} \quad (51)$$

B. Coupled superconducting \mathbb{Z}_3 Rabi models

It is straightforward to implement the Potts model based on superconducting circuits. We consider a chain of superconducting circuits depicted in Fig. 3. Next, we need to couple the neighbor Rabi models with a boson hopping term to get the Hamiltonian (46). To do it, we couple the neighbor Rabi models using inductors (Fig. 5). Despite being more common, the capacitor coupling

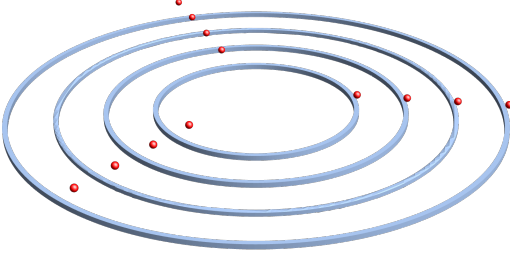


FIG. 6. Schematic illustration of the optomechanical (OM) implementation of the Potts model. It consists of several concentric OM implementations of the Rabi model, i.e., several concentric cyclic chiral waveguide and three trapped ions on top of each waveguide.

does not work in our case because it leads to all-to-all coupling between the Rabi models after the circuit quantization.

On the other hand, the inductor coupling leads us to the hopping term we want. First of all, the Hamiltonian terms corresponding to the inductors are:

$$\hat{V}_{\text{Potts},n} = \frac{1}{2L_{\text{Potts}}}(\hat{\phi}_{n+1} - \hat{\phi}_n)^2 = \frac{(\hat{\phi}_n^2 + \hat{\phi}_{n+1}^2)}{2L_{\text{Potts}}} + \frac{\hat{a}_n^\dagger \hat{a}_{n+1}^\dagger + \hat{a}_n^\dagger \hat{a}_{n+1} + \hat{a}_n \hat{a}_{n+1}^\dagger + \hat{a}_n \hat{a}_{n+1}}{L_{\text{Potts}} C_B \Omega_{QB}} \quad (52)$$

where we expressed the flux operator through the creation/annihilation operators $\hat{\phi}_n = (\hat{a}_n + \hat{a}_n^\dagger)/\sqrt{2C_B\Omega_{QB}}$.

We ignore the $\hat{\phi}_n^2$ and $\hat{\phi}_{n+1}^2$ terms because they simply renormalize the Rabi model parameters. Additionally, the inductor coupling produces undesired terms $\hat{a}_n^\dagger \hat{a}_{n+1}^\dagger$ and $\hat{a}_n \hat{a}_{n+1}$. However, we can use Rotating Wave Approximation (RWA) to eliminate them. For the RWA to be applicable, we need $\Omega_{QB} = \sqrt{L_B C_B} \gg (L_{\text{Potts}} C_B \Omega_{QB})^{-1}$. After RWA we are left with the hopping term between the boson modes of the neighbor Rabi model. Consequently, in line with Sec. V A the superconducting circuit in question is modeled by the Potts model. The coupling parameters of the resulting Potts model could be expressed through the circuit parameters:

$$f_{\text{Potts}} = \frac{I_{\text{Rabi}}}{2} \exp\left(-\frac{1}{2} \sqrt{\frac{L_B}{C_B}}\right), \quad (53)$$

$$J_{\text{Potts}} = \frac{1}{2L_{\text{Potts}}} \sqrt{\frac{L_B}{C_B}}.$$

C. Coupled optomechanical \mathbb{Z}_3 Rabi models

We can repeat the same procedure for the optomechanical system. However, it is a bit more peculiar, because of the circular waveguide in the optomechanical Rabi model. To build the optomechanical \mathbb{Z}_3 Potts model we

arrange the optomechanical \mathbb{Z}_3 Rabi model concentrically (see Fig. 6). On the one hand, the radius of the waveguide does not affect the parameters of the model, on the other hand, placing the ions of the neighbor Rabi models close to each other creates phonon-phonon interaction through the ion Coulomb interaction [? ?]. The phonon-phonon interaction between the neighboring Rabi models leads to the Hamiltonian (46) and consequently to the \mathbb{Z}_3 Potts model as described before.

D. Chiral Potts model and parafermions

In this subsection, we want to briefly overview the chiral Potts model. It is a generalization of the ordinary Potts model that has a chiral nearest-neighbour interaction:

$$H_{\text{chPotts}} = f' \sum_{n=1}^L (e^{i\phi'} Z_n + e^{-i\phi'} Z_n^\dagger) + J' \sum (e^{i\theta'} X_n X_{n+1}^\dagger + e^{-i\theta'} X_n^\dagger X_{n+1}). \quad (54)$$

In other words, it is the Potts model (45) with a complex parameter J' .

The chiral Potts model exhibits richer physics compared to the ordinary one. In particular, it can host parafermion physics. We talk more about it below, but first, we need to discuss how to obtain this chiral interaction, because it is quite challenging.

As mentioned earlier, the interaction parameter J' originates from the neighbor \mathbb{Z}_3 Rabi models boson interaction. Hence, if we want to obtain the chiral Potts model, we have to obtain a chiral boson-hopping term. The full technical discussion of this topic is outside of this paper's scope. However, we want to mention that recently a way to obtain the chiral boson hopping was proposed in [?], and we assume that it could be adapted to our system.

For the Potts system a certain generalization of the Jordan-Wigner transformation exists. It is called the Fradkin-Kadanoff (FK) transformation [?], and it allows us to rewrite X_j, Z_j in terms of parafermions:

$$\Gamma_j = \prod_{k < j} Z_k X_j, \quad \Delta_j = \prod_{k \leq j} Z_k X_j. \quad (55)$$

Here Γ_j, Δ_j are parafermion operators with a parafermion commutation relation: $\Gamma_j \Gamma_k = \omega^{\text{sign}(j-k)} \Gamma_k \Gamma_j$, $\Delta_j \Delta_k = \omega^{\text{sign}(j-k)} \Delta_k \Delta_j$, and finally $\Gamma_j \Delta_k = \omega^{\text{sign}(j-k)} \Delta_k \Gamma_j$.

Using the FK transformation, it is easy to show that the Potts model is equivalent to a parafermion chain. The only problem is that FK transformation is not local. In terms of parafermion operators, the chiral Potts model Hamiltonian (54) looks like

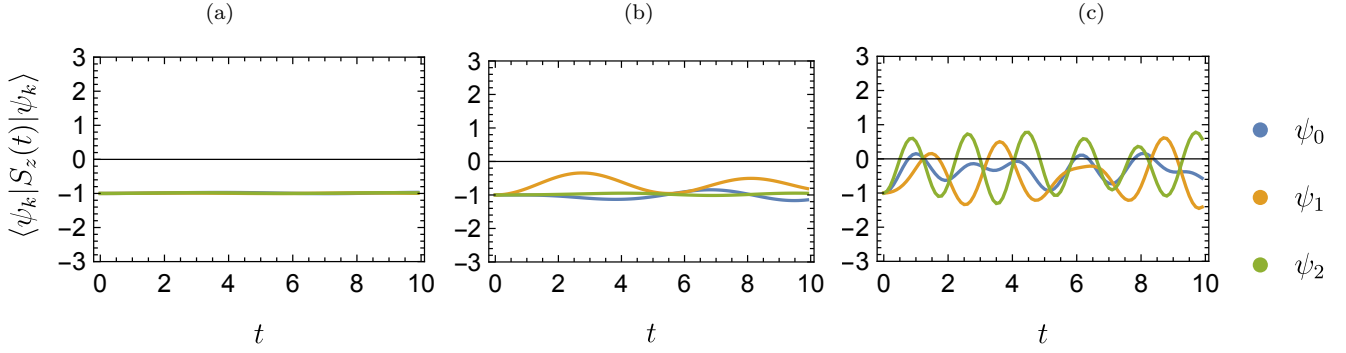


FIG. 7. Time dependence of the total spin excitation operator. To illustrate robustness of the Rabi model implementation with the respect of disorder (59) we plotted $\langle S_z(t) \rangle$. The standard variance of the disorder Δ_j equals for plot a) 0.1; b) 0.3; c) 1.

$$H_{\text{chPotts}} = f' \sum \left(e^{i\phi'} \Gamma_j \Delta_j^\dagger + e^{-i\phi'} \Delta_j \Gamma_j^\dagger \right) + J' \sum \left(e^{i\theta'} \Delta_j \Gamma_{j+1}^\dagger + e^{-i\theta'} \Gamma_{j+1} \Delta_j^\dagger \right) \quad (56)$$

On the other hand, it is known that parafermion chain has a phase with a parafermion edge mode [?]:

$$\Gamma_{\text{edge}} = \Gamma_1 + \frac{f'}{J' \sin(3\theta')} \mathcal{O} + \dots \quad (57)$$

Unfortunately, after the parafermion edge mode is not localized on the edged after FK transformation. As a result, we do not have an actual topological phase in the chiral Potts model. But we believe that it still holds an importance because it allows us to simulate a parafermion chain.

VI. DISORDER IN THE SUPERCONDUCTING IMPLEMENTATION

A. Disorder breaking the total qubit excitation number conservation

First, while discussing the effect of the disorder on the qubit-boson ring (28), we need to consider a term that breaks the conservation of the total excitation number of qubits \hat{S}^z . This conservation law is broken by the Zeeman terms being not perfectly aligned with \hat{z} direction:

$$\hat{H}_{QB,\text{dis}} = \hat{H}_{QB} + \sum_{j=1}^3 \Delta_j \sigma_j^x. \quad (58)$$

As explained in App. 9, Δ_j being equal to zero for qubit-boson ring based on superconducting circuits relies on the fine-tuning of the SQUID magnetic field. Therefore, in a realistic setting we unavoidably are going to have non-zero $\Delta_j = I_{Q,1} \sin(\Delta\Phi_j)$.

As a result, we have $[\hat{H}_{QB,\text{dis}}, \hat{S}^z] \neq 0$. Unfortunately, it breaks the derivation of the Rabi model. However,

assuming that the disorder is considerably smaller than other parameters in the Hamiltonian, we can still hope that the dynamics is approximately governed by the Rabi model. Because an analytic estimate is cumbersome, we performed numerical simulations of the qubit-boson ring. The results could be seen on Fig. 7. The simulation shows that for the small disorder the qubit-boson ring stays around the single excitation subspace \mathcal{H}_1 because $\langle \hat{S}^z \rangle(t) \approx 1$. We speculate that it happens because the spins precess around $\langle \hat{S}^z \rangle = 1$.

B. Disorder breaking \mathbb{Z}_3 symmetry

Now, assuming that the total number of qubit excitations is conserved, we would like to investigate how the coordinate dependence of the parameter in the qubit-boson ring influences the resulting Rabi model. The spatial non-homogeneity obviously breaks the \mathbb{Z}_3 symmetry. However, we want to find the explicit symmetry-breaking term.

$$\begin{aligned} \hat{H}'_{QB} = & \sum_j \epsilon_j \sigma_j^z + \sum_j \Omega_j \hat{a}_j^\dagger \hat{a}_j \\ & + \sum_j g_{j,j+1} \left[\sigma_j^+ \sigma_{j+1}^- e^{i(\hat{x}_j - \hat{x}_{j+1})} + \text{h.c.} \right] \end{aligned} \quad (59)$$

where we have

$$\begin{aligned} \epsilon_j &= \frac{\delta_j}{2C_{Q,j}}, \quad \Omega_{QB,j} = (L_{B,j} C_{B,j})^{-1/2}, \\ g_{j,j+1} &= \frac{I_{\text{Rabi},j}}{2}. \end{aligned} \quad (60)$$

For brevity, we decompose the coupling parameters into a homogeneous part and a disorder: $\epsilon_j = \epsilon + \Delta\epsilon_j$, $\Omega_j = \Omega + \Delta\Omega_j$, $g_{j,j+1} = g + \Delta g_{j,j+1}$, where we assume that the disorder averaged over the coordinate is zero: $\sum_j \Delta\epsilon_j = \sum_j \Delta\Omega_j = \sum_j \Delta g_{j,j+1} = 0$. We can always achieve this by adjusting the homogeneous coupling.

Then the single-excitation sector is going to be de-

scribed by

$$\begin{aligned}
\hat{H}'_{2 \text{ Rabi}} &= \hat{H}_{2 \text{ Rabi}} + \epsilon(2)X \\
&+ \epsilon(1)X^\dagger + (X + X^\dagger) \sum_{k=1}^2 \Delta g(k)Z^k \\
&+ \Omega(1) \sum_{k=0}^2 \hat{a}^\dagger(k+1)\hat{a}(k) + \Omega(2) \sum_{k=0}^2 \hat{a}^\dagger(k)\hat{a}(k+1) \quad (61) \\
&+ \sum_{l=1}^2 \frac{\Omega^{3/2}(l)}{2^{3/2}} \sum_{k=0}^2 (\hat{a}(k+l) + \hat{a}^\dagger(-k-l))Z^k.
\end{aligned}$$

Due to the disorder the first boson mode does not decouple anymore. However, the structure of threefold cat state should be still conserved for small disorder.

VII. CONCLUSION

In this paper, we explored several models with the \mathbb{Z}_3 symmetry, with a particular focus on the \mathbb{Z}_3 Rabi model and its variations. By employing a canonical transformation, we successfully derived the spectrum of these models, revealing that the three lowest eigenstates correspond to distinct threefold cat states, a feature interesting from several perspectives. We derived an analytical expression for the Wigner quasi-probability function of the threefold cat state and used it to better understand the structure of the cat states.

We also introduced a hierarchy of \mathbb{Z}_3 -symmetric systems. In the qubit-boson ring, the \mathbb{Z}_3 symmetry appears as a discrete rotational symmetry, whereas in the Rabi model, a specific sector of the qubit-boson ring, the symmetry acts as an internal one. This internal symmetry also exists in the \mathbb{Z}_3 Potts model, which we constructed by coupling multiple \mathbb{Z}_3 Rabi models.

Our main goal was to suggest a way towards an experimental realization of the \mathbb{Z}_3 Rabi and Potts models. We believe that the proposed superconducting circuit should be feasible to implement. However, this approach does not have to be restricted only to the superconducting circuit platform. For example, we believe that a similar strategy work for the spin-qubit systems. Though, this remains a topic for a future research.

More broadly, our work highlights the intriguing potential of \mathbb{Z}_n -symmetric systems within condensed matter physics. These systems present a fertile ground for discovering novel quantum phenomena, many of which are yet to be fully understood or described. We believe that further investigation into these models will reveal new insights and advance our understanding of symmetry in quantum systems.

ACKNOWLEDGMENTS

We thank Daria Kalacheva, Henry Legg, Katharina Laubscher, and Ilia Luchnikov for fruitful discussions and

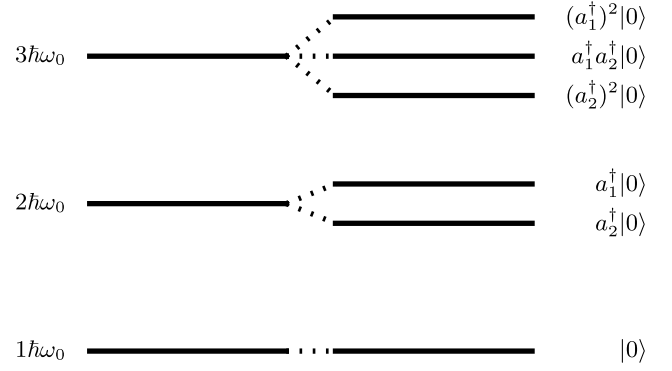


FIG. 8. Eigenvalue degeneracy of 2-dimensional quantum harmonic oscillator.

useful comments. This work was supported as a part of NCCR SPIN, a National Centre of Competence in Research, funded by the Swiss National Science Foundation (grant number 225153). This work has received funding from the Swiss State Secretariat for Education, Research and Innovation (SERI) under contract number M822.00078.

Appendix A: $SU(2)$ symmetry in 2-dimensional quantum harmonics oscillator

Despite the 2-dimensional quantum harmonic oscillator (2d QHO) being discussed in any introductory quantum mechanics course, we still would like to briefly review a certain fact related to 2d QHO. Its Hamiltonian is

$$\hat{H} = \Omega(\hat{a}_1^\dagger \hat{a}_1 + \hat{a}_2^\dagger \hat{a}_2 + 1). \quad (A1)$$

It basically counts the number of excitations in the both QHOs. Keeping in mind that the 1-dimensional QHO eigenenergies are just $\hbar\Omega(n + 1/2)$, we can easily deduce the spectrum of 2d QHO. We now have 2 modes, in which we can put additional excitations. As a result, the n th eigenenergy becomes degenerate. Using the basic combinatorial fact that there are $(n+1)$ ways to divide n objects into 2 groups, it follows that the n th energy level has $(n+1)$ -fold degeneracy. This looks quite similar to the $SU(2)$ group representations, i.e. there is exactly one $SU(2)$ representation on a n -dimensional vector space. Indeed, it turns out to be not a coincidence: 2d QHO has a $SU(2)$ symmetry which “rotates” the excitations between different axes.

The explicit expressions for the generators are easily provided:

$$\begin{aligned}
\hat{L}_1 &= \hat{a}_1^\dagger \hat{a}_2 + \hat{a}_2^\dagger \hat{a}_1, \\
\hat{L}_2 &= i\hat{a}_1^\dagger \hat{a}_2 - i\hat{a}_2^\dagger \hat{a}_1, \\
\hat{L}_3 &= \hat{a}_1^\dagger \hat{a}_1 - \hat{a}_2^\dagger \hat{a}_2.
\end{aligned} \quad (A2)$$

Despite being a rather trivial fact, the presence of the $SU(2)$ symmetry is relevant in our discussion of the 2-

mode \mathbb{Z}_n Rabi model, which is a 2d QHO oscillator coupled with an n -level system. The interaction between the 2d QHO and the n -level system can either break an $SU(2)$ symmetry, or conserve it. As a result, we find the discussion of the $SU(2)$ symmetry quite important for our purposes.

Appendix B: Alternative 2-mode \mathbb{Z}_3 Rabi model

In this appendix, we examine a straightforward 2-mode extension of the \mathbb{Z}_3 Rabi model (5). We simply double the number of boson modes without altering the Hamiltonian in any other way:

$$\hat{H} = \Omega(\hat{a}_1^\dagger \hat{a}_1 + \hat{a}_2^\dagger \hat{a}_2) + B(e^{i\phi} Z + e^{-i\phi} Z^\dagger) - \lambda \left[(\hat{a}_1^\dagger + \hat{a}_2^\dagger) X + (\hat{a}_1 + \hat{a}_2) X^\dagger \right] \quad (\text{B1})$$

Correspondingly, the \mathbb{Z}_3 symmetry generator is

$$\hat{R} = \exp\left[\frac{2\pi i}{3} \hat{N}\right] \cdot Z, \text{ with } \hat{N} = \hat{a}_1^\dagger \hat{a}_1 + \hat{a}_2^\dagger \hat{a}_2. \quad (\text{B2})$$

However, we still have the $SU(2)$ symmetry of the 2d QHO left. As a result, in this system we have \mathbb{Z}_3 and $SU(2)$ symmetries combined into $G = \mathbb{Z}_3 \times SU(2)$. It leads to a degeneracy of the eigenvalues similar to the one we saw in App. A. In this sense, the second mode addition did not change anything but the multiplicity of the eigenenergies. As a consequence, we find the 2-mode \mathbb{Z}_3 Rabi model discussed in Sec. III to be more interesting compared to this one.

Appendix C: Qubit-boson ring with an arbitrary matrix interaction

In Sec. IV A we proposed to physically implement the \mathbb{Z}_3 Rabi model using the spin-boson ring with the special interaction (28). The main idea is that the \mathbb{Z}_3 Rabi model describes the dynamics of the spin-boson ring in the single excitation sector \mathcal{H}_1 , i.e., the subspace of the Hilbert space \mathcal{H} with a single spin up. In this appendix, we discuss this idea more thoroughly. In particular, we consider a more general Hamiltonian that simultaneously represents the superconducting qubit implementation, described in Sec. IV B, and the optomechanical implementation, described in Sec. IV C. For this purpose, we add an interaction matrix A that describes the relative strength of spin-qubit interaction V_{gen} between different sites. Specifically, the interaction matrix A describes the connectivity of the model.

$$\begin{aligned} \hat{H}_{\text{gen}} &= \epsilon \sum_{j=1}^3 \sigma_i^z + \Omega \sum_{j=1}^3 \hat{a}_j^\dagger \hat{a}_j + \hat{V}_{\text{gen}}, \text{ with} \\ \hat{V}_{\text{gen}} &= g \sum_{j,k} A_{jk} \sigma_j^+ \sigma_k^- e^{i\eta(\hat{x}_j - \hat{x}_k)}, \end{aligned} \quad (\text{C1})$$

where A_{jk} is an $n \times n$ matrix with $A^\dagger = A$ by virtue of \hat{V} being Hermitian. The matrix A basically describes the connectivity of the model and the relative strength of different interaction terms. In case of $A_{jk} = \delta_{j-1,k} + \delta_{j+1,k}$ and $\eta = 1$ the model (C1) is reduced to the one (28) considered in the main text. In fact, we can eliminate η by rescaling the coordinate and momentum operators. Although physically it corresponds to the time scaling and changes the boson mass $m \rightarrow m/\eta^2$, we employ this transformation to make the following treatment more uniform.

The Hamiltonian commutes with the total number of spin excitations operator $\hat{S}^z = \sum_j \sigma_j^z$. Hence, the number of spin excitations is conserved, and it is possible to decompose the Hilbert space into sectors with a fixed number of spin excitations $\mathcal{H} = \mathcal{H}_0 \oplus \mathcal{H}_1 \oplus \mathcal{H}_2 \oplus \mathcal{H}_3$. For each sector we have $\hat{S}^z|_{\mathcal{H}_n} = (2n - 3) \text{Id}_{\mathcal{H}_n}$.

To prove that the \mathbb{Z}_3 Rabi model describes the dynamics of (C1) in the single spin excitation sector \mathcal{H}_1 we first need to transform the Hamiltonian a bit. The short plan is to apply a spin-dependent momentum translation. Afterwards, we apply the Fourier transform, and finally restrict the model to a single excitation subspace. In the end, we obtain the \mathbb{Z}_3 Rabi model.

First of all, we would like to apply the unitary transformation $\hat{S} = \prod_j \exp[i\sigma_j^z \eta \hat{x}_j / 2]$. Considering that $\exp[ia\hat{x}]$ is a momentum translation operator, one can interpret \hat{S} as a spin-dependent momentum translation. Its purpose is to make \hat{V}_{gen} an interaction acting purely on the spin degrees of freedom. In place of it we obtain a simpler interaction between the spin and the boson degrees of freedom $\sum_j \hat{p}_j \sigma_j^z$:

$$\begin{aligned} S^{-1} \hat{H}_{\text{gen}} S &= \epsilon \sum \sigma_i^z + \Omega \sum \hat{a}_j^\dagger \hat{a}_j + \frac{1}{2m} \sum \hat{p}_j \sigma_j^z + \frac{n}{4m} \\ &\quad + g \sum_{j,k} A_{jk} \sigma_j^+ \sigma_k^-. \end{aligned} \quad (\text{C2})$$

As a next step, we apply the Fourier transform to the spin and boson operators. Despite working explicitly with a system of length 3, we define the Fourier transform in a general case of length N system, because it is clearer this way. The Fourier transform for the observable \hat{O} , e.g., $\hat{\sigma}^z, \hat{x}, \hat{p}, \dots$, is

$$\hat{O}(k) = \frac{1}{\sqrt{N}} \sum_{j=1}^N e^{-\frac{2\pi i}{N} k j} \hat{O}_j, \quad (\text{C3})$$

where $k = 0, 2\pi/N, \dots, (N-1) \cdot 2\pi/N$ is a wavevector.

Consequently, for the momentum operators in the reciprocal space we have

$$\hat{p}(k) = i\sqrt{\frac{m\Omega}{2}} (-\hat{a}(k) + \hat{a}^\dagger(-k)) \quad (\text{C4})$$

However, this convention changes the commutation relations a bit: $[\hat{x}(k_1), \hat{p}(k_2)] = i\delta_{k_1, -k_2}$, while $[\hat{a}(k_1), \hat{a}^\dagger(k_2)] = \delta_{k_1, k_2}$.

Spin operators after the Fourier transform are convenient for several reasons. For example, $\sigma^z(0)$ is a total excitation number operator. Thanks to it being conserved, the zeroth boson component is decoupled from the rest of the system. Moreover, the restriction of $\sigma^z(k)$ to the single excitation subspace \mathcal{H}_1 is simple:

$$\sigma^z(k) \Big|_{\mathcal{H}_1} = \frac{2 - 3\delta_{k,0}}{\sqrt{3}} Z^k. \quad (\text{C5})$$

We do not apply the discrete Fourier transform to $S^{-1}\hat{V}_{\text{gen}}S$, because it is already in a convenient form to restrict it to the single excitation subspace. Taking the all aforementioned details into the account we arrive at:

$$\begin{aligned} S^{-1}\hat{H}_{\text{gen}}S &= \epsilon\sigma^z(0) + \Omega \sum_{k=0}^2 \hat{a}^\dagger(k)\hat{a}(k) \\ &+ \frac{i}{2}\sqrt{\frac{\Omega}{2m}} \sum_{k=0}^2 (-\hat{a}(k) + \hat{a}^\dagger(-k))\sigma^z(k) \quad (\text{C6}) \\ &+ \frac{N}{4m} + g \sum_{j_1, j_2=1}^3 A_{j_1 j_2} \sigma_{j_1}^+ \sigma_{j_2}^-. \end{aligned}$$

Now we can safely restrict the Hamiltonian to the subspace \mathcal{H}_1 . It does not affect boson operators, and the spin operators restriction we have already discussed. As a result, the Hamiltonian reaches a form quite similar to the \mathbb{Z}_3 Rabi model (20):

$$\begin{aligned} S^{-1}\hat{H}_{\text{gen}}S \Big|_{\mathcal{H}_1} &= \epsilon + \frac{N}{4m} + gA \\ &+ \Omega \hat{a}^\dagger(0)\hat{a}(0) - \frac{i}{2}\sqrt{\frac{\Omega}{6m}} (-\hat{a}^\dagger(0) + \hat{a}(0)) \\ &+ \Omega [\hat{a}^\dagger(1)\hat{a}(1) + \hat{a}^\dagger(2)\hat{a}(2)] \\ &+ i\sqrt{\frac{\Omega}{6m}} [(-\hat{a}(1) + \hat{a}^\dagger(2))Z + (-\hat{a}(2) + \hat{a}^\dagger(1))Z^\dagger], \end{aligned} \quad (\text{C7})$$

where matrix A became operator acting in \mathcal{H}_1 .

We drop the first line in Hamiltonian, because it contains only constants and the decoupled boson mode $\hat{a}_0, \hat{a}_0^\dagger$. As a next step, we apply Hadamard transform $\hat{H}_{ij} = \omega^{i-j}/\sqrt{3}$ to \mathcal{H}_1 to turn Z, Z^2 operators in the spin-boson interaction term into X, X^2 operators. Also, we employ the quantum harmonic oscillator $U(1)$ phase symmetry to get rid of the imaginary unit in front of the interaction term ($\hat{a}(k) \mapsto -i\hat{a}(k)$, $\hat{a}^\dagger(k) \mapsto i\hat{a}^\dagger(k)$):

$$\begin{aligned} \hat{H} &= \Omega [\hat{a}^\dagger(1)\hat{a}(1) + \hat{a}^\dagger(2)\hat{a}(2)] \\ &- \sqrt{\frac{\Omega}{6m}} [(\hat{a}(1) + \hat{a}^\dagger(2))\hat{X} + (\hat{a}(2) + \hat{a}^\dagger(1))\hat{X}^\dagger] \quad (\text{C8}) \\ &+ g\hat{H}\hat{A}\hat{H}^{-1} \end{aligned}$$

We already arrived to the \mathbb{Z}_3 Rabi model. If we remember about time scaling we used to get rid of η , we

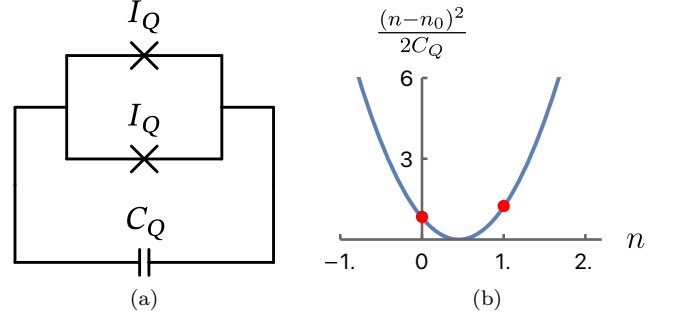


FIG. 9. Second-harmonic qubit. a) The electric circuit of the second-harmonic qubit circuit. b) The capacitor potential (D4) for $n_0 = 0.45 = 0.5 - 0.05$. The red dots show the eigenenergies of the second-harmonic qubit.

can write down the following expressions for the Rabi model parameters:

$$\Omega_R = \Omega, \quad \lambda = \sqrt{\frac{\Omega\eta^2}{6m}}. \quad (\text{C9})$$

However, the purely spin term is expressed by an arbitrary interaction matrix A . The \mathbb{Z}_3 symmetry puts a restriction on the form of A . The both superconducting qubit and optomechanical cases we are interested in satisfy this requirement. Consequently, they could be transformed to the canonical 2-mode \mathbb{Z}_3 Rabi model (20).

Now in the case of the superconducting qubit platform we simply have $A = X + X^2$. Substituting it into (C8), we obtain precisely the \mathbb{Z}_3 Rabi model:

$$\begin{aligned} \hat{H} &= g(Z + Z^2) + \Omega [\hat{a}^\dagger(1)\hat{a}(1) + \hat{a}^\dagger(2)\hat{a}(2)] \\ &- \sqrt{\frac{\Omega}{2m}} [(\hat{a}(1) + \hat{a}^\dagger(2))X + (\hat{a}(2) + \hat{a}^\dagger(1))X^\dagger] \end{aligned} \quad (\text{C10})$$

In the optomechanical case the form of the interaction matrix A is a bit more complicated

$$A = \begin{pmatrix} 0 & i & i \\ -i & 0 & i \\ -i & -i & 0 \end{pmatrix}. \quad (\text{C11})$$

Consequently, we need to apply an additional transformation defined by matrix $U_{ij} = \exp[2\pi i(3/2 - j)(i - 1)/3]/\sqrt{3}$. In the end, we arrive at

$$\begin{aligned} U^\dagger \hat{H} U &= g(e^{-5\pi i/6}Z + e^{5\pi i/6}Z^2) \\ &+ \Omega [\hat{a}^\dagger(1)\hat{a}(1) + \hat{a}^\dagger(2)\hat{a}(2)] \\ &- \sqrt{\frac{\Omega}{2m}} [(\hat{a}(1) + \hat{a}^\dagger(2))X + (\hat{a}(2) + \hat{a}^\dagger(1))X^\dagger] \end{aligned} \quad (\text{C12})$$

In general, the same procedure is possible for any qubit-boson ring (C1) with a \mathbb{Z}_3 symmetric matrix A .

Appendix D: Charge qubit for the \mathbb{Z}_3 Rabi model

The Cooper Pair Box (CPB) qubit is the most well-known type of charge qubit. However, it is not suitable for our purposes because its eigenstates are not charge states but their symmetric/antisymmetric combinations. In other words, its Hamiltonian is proportional to σ^x . But in this case, the qubit chain Hamiltonian does not commute with total number of qubit excitations operator S^z .

Hence, we need another type of a charge qubit. Considering that the σ^x term in the Hamiltonian arises from the JJ term the natural idea is to get rid of the JJ and consider a purely capacitor qubit. Although theoretically suitable for our purposes, without the JJ the charge qubit is very sensitive to noise. Therefore, it is not a realistic approach.

Consequently, we want two things simultaneously: Hamiltonian proportional to σ^z in charge basis and JJ to fight noise. The solution turns out to be a higher harmonic Josephson junction. Usually it is neglected, but the JJ Hamiltonian always include higher harmonics as well

$$\hat{H}_{JJ} = E_{J,1} \cos \hat{\phi} + E_{J,2} \cos 2\hat{\phi} + \dots, \quad (\text{D1})$$

where ϕ is the superconducting phase.

In practice, the higher harmonics are usually considerably weaker $E_{J,2} \ll E_{J,1}$. But if we were to kill the first harmonic completely, then we would be left with the second harmonic. The second harmonic, on the one hand, can help to suppress the noise and, on the other hand,

does not appear in the qubit Hamiltonian:

$$\cos 2\hat{\phi} \Big|_{\nu} = \frac{1}{2} \left(e^{2i\hat{\phi}} + e^{-2i\hat{\phi}} \right) \Big|_{\nu} = \frac{1}{2} ((\sigma^+)^2 + (\sigma^-)^2) = 0 \quad (\text{D2})$$

To eliminate the first harmonic, we can use a Superconducting Quantum Interference Device (SQUID) [?]. If the magnetic flux through the SQUID is tuned to $\Phi = \pi$, then the SQUID Hamiltonian will look like:

$$\begin{aligned} \hat{H}_{\text{squid}} = & I_{Q,1} \cos \hat{\phi} + I_{Q,2} \cos 2\hat{\phi} + I_{Q,1} \cos(\hat{\phi} + \pi) \\ & + I_{Q,2} \cos(2\hat{\phi} + 2\pi) = 2I_{Q,2} \cos 2\hat{\phi}. \end{aligned} \quad (\text{D3})$$

As a result, only the second harmonic is left.

Consequently, we can construct a qubit based on the second-harmonic JJ (see Fig. 9). It is described by the Hamiltonian:

$$\hat{H} = \frac{1}{2C_Q} (\hat{n} - n_0)^2 + 2I_{Q,2} \cos 2\hat{\phi} \quad (\text{D4})$$

If we tune n_0 a bit off $1/2$: $n_0 = 0.5 - \delta$, then the qubit Hamiltonian will look like:

$$\hat{H}_{\text{qubit}} = \frac{\delta}{2C_Q} \sigma_z. \quad (\text{D5})$$

Hence, we obtained the qubit Hamiltonian we wanted. Here we consider $\frac{1}{2C} \gg 2E_{J,2}$ as usual for charge qubits.

To conclude, the charge qubit we have in mind consists of a capacitor and the second-harmonic JJ. One can think of it as a certain generalization of a Cooper Pair Box qubit. In this appendix, we only briefly described its blueprint to give additional substance to the proposal in Sec. IV B.